Microscopic nucleon spectral function for finite nuclei featuring two- and three-nucleon short-range correlations: The model versus *ab initio* calculations for three-nucleon systems

Claudio Ciofi degli Atti,[1,*] Chiara Benedetta Mezzetti,[2,†] and Hiko Morita[3,‡]

[1]*Istituto Nazionale di Fisica Nucleare, Sezione di Perugia, c/o Department of Physics and Geology, University of Perugia,*
Via A. Pascoli, I-06123 Perugia, Italy
[2]*NiPS Laboratory, Department of Physics and Geology, University of Perugia, Via A. Pascoli, I-06123 Perugia, Italy*
[3]*Sapporo Gakuin University, Bunkyo-dai 11, Ebetsu 069-8555, Hokkaido, Japan*

Background: Two-nucleon ($2N$) short-range correlations (SRC) in nuclei have been recently thoroughly investigated, both theoretically and experimentally and the study of three-nucleon ($3N$) SRC, which could provide important information on short-range hadronic structure, is underway. Novel theoretical ideas concerning $2N$ and $3N$ SRC are put forward in the present paper.

Purpose: The general features of a microscopic one-nucleon spectral function which includes the effects of both $2N$ and $3N$ SRC and its comparison with *ab initio* spectral functions of the three-nucleon systems are illustrated.

Methods: A microscopic and parameter-free one-nucleon spectral function expressed in terms of a convolution integral involving *ab initio* relative and center-of-mass (c.m.) momentum distributions of a $2N$ pair and aimed at describing two- and three-nucleon short-range correlations, is obtained by using: (i) the two-nucleon momentum distributions obtained within *ab initio* approaches based upon nucleon-nucleon interactions of the Argonne family; (ii) the exact relation between one- and two-nucleon momentum distributions; (iii) the fundamental property of factorization of the nuclear wave function at short internucleon ranges.

Results: The comparison between the *ab initio* spectral function of ^{3}He and the one based upon the convolution integral shows that when the latter contains only two-nucleon short-range correlations the removal energy location of the peaks and the region around them exhibited by the *ab initio* spectral function are correctly predicted, unlike the case of the high and low removal energy tails; the inclusion of the effects of three-nucleon correlations brings the convolution model spectral function in much better agreement with the *ab initio* one; it is also found that whereas the three-nucleon short-range correlations dominate the high energy removal energy tail of the spectral function, their effects on the one-nucleon momentum distribution are almost one order of magnitude less than the effect of two-nucleon short-range correlations.

Conclusions: The convolution model of the spectral function of the three-nucleon systems featuring both two- and three-nucleon short-range correlations and correctly depending upon the *ab initio* two-nucleon relative and center-of-mass momentum distributions provides in the correlation region a satisfactory approximation of the spectral function in a wide range of momentum and removal energy. The extension of the model to complex nuclei is expected to provide a realistic microscopic parameter-free model of the spectral function, whose properties are therefore governed by the features of realistic two-nucleon interactions and the momentum distributions in a given nucleus.

I. INTRODUCTION

The long-standing problem of the role played by short-range correlations (SRC) in atomic nuclei has been the object of intense activity in recent years both from the theoretical and the experimental points of view (see the review papers given in Ref. [1]). The experimental investigation of two-nucleon ($2N$) SRC has reached a high level of sophistication [2] and, at the same time, a series of theoretical papers, based upon different approaches, have clarified, both qualitatively and quantitatively, the role played by SRC in nuclei [3–9]. In particular, it has been demonstrated (see, e.g., [5–9]) that

$2N$ SRC arise from a universal and fundamental property of the nuclear wave function at short internucleon distances, namely, its factorization into a wave function describing the relative motion of a nucleon pair and a function describing the motion of the center of mass (c.m.) of the pair with respect to the "spectator" $(A - 2)$-nucleon system. Concerning the role of possible $3N$ SRC, although important contributions have already appeared (see, e.g., [10–12]), much remains to be done in order to fully understand their structure and their effects on other relevant nuclear quantities like, e.g., the one-nucleon momentum distributions and spectral function (SF). It is the aim of this paper to illustrate a realistic many-body approach to the effects of $2N$ and $3N$ SRC on the one-nucleon hole spectral function and momentum distributions, two quantities which play a primary role in the study of short-range effects in nuclei. Preliminary results along the line presented in this paper have been previously given in Ref. [13].

————
*ciofi@pg.infn.it
†chiara.mezzetti@unipg.it
‡hiko@webmail.sgu.ac.jp

II. THE DEFINITION OF THE NUCLEON SPECTRAL FUNCTION AND ITS DESCRIPTION IN THE SRC REGION BY THE CONVOLUTION MODEL

A. The nucleon hole spectral function

As is well known, the nucleon (N) hole spectral function $P_A^N(\mathbf{k}_1, E)$ represents the joint probability that when the nucleon "N" "N" (usually called the *active nucleon*) with momentum $\mathbf{k}_1$ is removed instantaneously from the ground state of the nucleus A, the nucleus ($A - 1$) (usually called the *spectator nucleus*) is left in the excited state

$E_{A-1}^* = E - E_{\min}$, where E is the so-called *removal energy* and $E_{\min} = M_{A-1} + m_N - M_A = |E_A| - |E_{A-1}|$ with E_A and E_{A-1} being the (negative) ground-state energy of nuclei A and $A - 1$, respectively. The hole spectral function, which takes into account the fact that nucleons in nuclei have not only a momentum distribution, but also a distribution in energy, is trivially related to a well-defined many-body quantity, namely the two-points Green's function (see, e.g., [14]). In this paper we use the following well-known representation of the SF $P_A^N(\mathbf{k}_1, E)$:

$$P_A^N(\mathbf{k}_1, E) = \frac{1}{2J+1} \sum_{M, \sigma_1} \left\langle \Psi_A^{JM} \middle| a_{\mathbf{k}_1 \sigma_1}^\dagger \delta(E - (\hat{H}_A - E_A)) a_{\mathbf{k}_1 \sigma_1} \middle| \Psi_A^{JM} \right\rangle \tag{1}$$

$$= \frac{1}{2J+1} \sum_{M, \sigma_1} \sum \int_f \left| \left\langle \Psi_{A-1}^f \middle| a_{\mathbf{k}_1 \sigma_1} \middle| \Psi_{JM}^A \right\rangle \right|^2 \delta\left(E - \left(E_{A-1}^f - E_A\right)\right) \tag{2}$$

$$= \frac{1}{2J+1} (2\pi)^{-3} \sum_{M, \sigma_1} \sum \int_f \left| \int d\mathbf{r}_1 e^{i\mathbf{k}_1 \cdot \mathbf{r}_1} G_f^{M\sigma_1}(\mathbf{r}_1) \right|^2 \delta\left(E - \left(E_{A-1}^f - E_A\right)\right), \tag{3}$$

where $a_{\mathbf{k}_1 \sigma_1}^\dagger$ ($a_{\mathbf{k}_1 \sigma_1}$) is the creation (annihilation) operator of a nucleon with momentum $\mathbf{k}_1$ and spin σ, $\hat{H}_A$ is the intrinsic Hamiltonian for A interacting nucleons, and the quantity

$$G_f^{M\sigma_1}(\mathbf{r}_1) = \left\langle \chi_{\sigma_1}^{1/2}, \Psi_{A-1}^f(\{\mathbf{x}\}_{A-1}) \middle| \Psi_A^{JM}(\mathbf{r}_1, \{\mathbf{x}\}_{A-1}) \right\rangle, \tag{4}$$

which has been obtained using the completeness relation for the eigenstates of the nucleus ($A - 1$) ($\sum_f |\Psi_{A-1}^f\rangle\langle\Psi_{A-1}^f| = 1$), is the overlap integral between the ground state wave function of nucleus A, Ψ_A^{JM}, and the wave functions of the discrete and all possible continuum eigenfunctions Ψ_{A-1}^f (with eigenvalue $E_{A-1}^f = E_{A-1} + E_{A-1}^{f*}$) of the nucleus ($A - 1$); eventually, $\{\mathbf{x}\}$ denotes the set of spin-isospin and radial coordinates. In what follows the angle integrated SF is normalized according to ($\mathbf{k}_1 \equiv \mathbf{k}, |\mathbf{k}| \equiv k$)

$$4\pi \int P_A^N(k, E) k^2 \, dk \, dE = 1. \tag{5}$$

and the momentum distribution (normalized to one) is linked to the SF by the *momentum sum rule*

$$\int P_A^N(k, E) \, dE = n_A^N(k). \tag{6}$$

Thanks to its very definition, the SF can be represented in the following useful form [8]:

$$P_A^N(k, E) = P_0^N(k, E) + P_1^N(k, E), \tag{7}$$

where P_0^N describes the shell-model part (with occupation probability of shell-model states less than one because of SRC populating the states above the Fermi level)

$$P_0^N(k, E) = (2\pi)^{-3} (2J+1)^{-1} \sum_{M, \sigma, f \leqslant F} \left| \int e^{i\mathbf{k}_1 \cdot \mathbf{r}_1} G_f^{M\sigma}(\mathbf{r}_1) \, d\mathbf{r}_1 \right|^2$$
$$\times \delta(E - E_{\min}), \tag{8}$$

and P_1^N describes the contribution from the discrete and continuum states above the Fermi level originating from ground-state SRC

$$P_1^N(k, E) = (2\pi)^{-3} (2J+1)^{-1}$$
$$\times \sum_{M, \sigma} \sum_{f > F} \int \left| \int e^{i\mathbf{k}_1 \cdot \mathbf{r}_1} G_f^{M\sigma}(\mathbf{r}_1) \, d\vec{r}_1 \right|^2$$
$$\times \delta\left(E - E_{A-1}^f\right). \tag{9}$$

B. The *ab initio* spectral function of ³He: The plane wave impulse approximation (PWIA) vs the plane wave approximation (PWA)

Due to the summation over the entire spectrum of states of the final nucleus, the exact (*ab initio*) spectral function can only be calculated for the three-nucleon systems for which only two final states are open, namely the deuteron and the continuum two-nucleon states. For this reason in this paper we will consider the case of mirror nuclei with $A = 3$, which are described by two different spectral functions and momentum distributions, namely the proton (p) and the neutron (n) ones, which are defined as follows:

$$P_3^{p(n)}(k, E) = P_{gr}^{p(n)}(k, E) + P_{ex}^{p(n)}(k, E), \tag{10}$$

for the proton (neutron) spectral function in ³He (³H), and

$$P_3^{p(n)}(|\mathbf{k}_1|, E) = P_{ex}^{p(n)}(|\mathbf{k}_1|, E), \tag{11}$$

for the proton (neutron) spectral function in ³H(³He). In both nuclei the ground (gr) part, has the following form:

$$P_{gr}^{p(n)}(|\mathbf{k}_1|, E) = n_{gr}^{p(n)}(|\mathbf{k}_1|) \delta(E - E_{\min}), \tag{12}$$

where $E_{\min} = |E_3| - |E_2| \approx 5.49 \, \text{MeV}$ and $n_{gr}^{p(n)}(|\mathbf{k}_1| \equiv k_1)$ is the momentum distribution corresponding to the
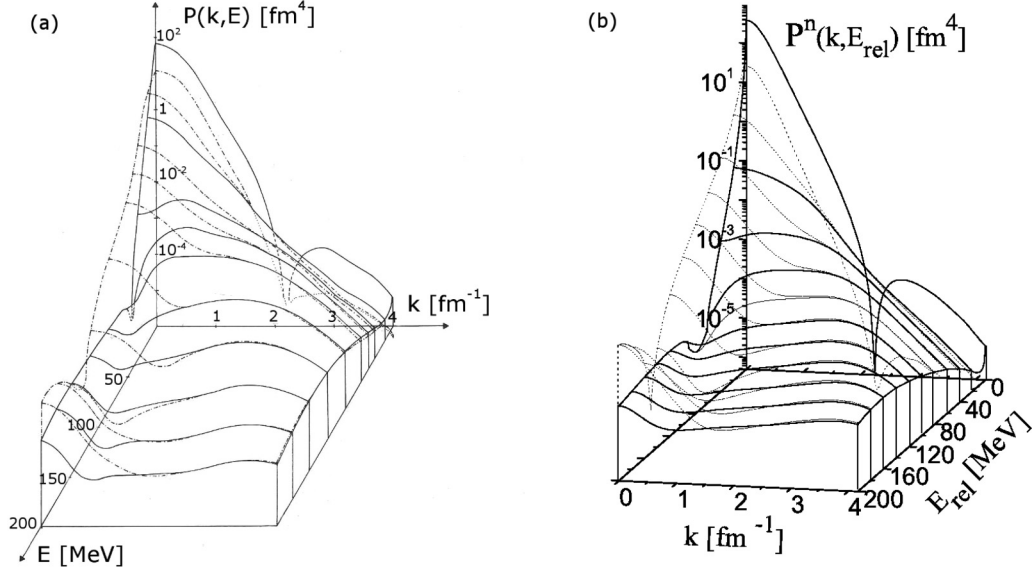
FIG. 1. The *ab initio* neutron spectral function of ^{3}He [Eq. (14)] calculated in Ref. [15] using $3N$ wave functions corresponding to the RSC interaction [16] (a) and in Ref. [17] using $3N$ wave functions [18] corresponding to the AV18 [19] interaction (b). In both cases the full lines represent the PWIA (the proton-proton wave function $\Psi_{pp}^{\mathbf{t}}$ in the final state is the exact solution of the the Hamiltonian which has been used to obtain the ground-state wave function), whereas the dot-dashed line in (a) and the dotted line in (b) correspond to the PWA (the final pp state is approximated by a plane wave). The regions where the PWA practically coincides with the PWIA are clearly visible and correspond to high values of the momentum. In (b) $E_{\rm rel} = E + |E_3|$, $|E_3|$ being the binding energy of ^{3}He and $E_{\rm rel}$ is the relative energy of the proton-proton pair in the continuum. Therefore the energy scales in the two Figures differ only by the small value $|E_3| = 7.718$ MeV.

two-body break-up (2bbu) channel $^3{\rm He} \to D + p$ ($^3{\rm H} \to D + n$), namely,

$$n_{gr}^{p(n)}(k) = \frac{1}{(2\pi)^3} \frac{1}{2} \sum_{M_D, M_3, \sigma_1} \left| \int e^{-i\boldsymbol{\rho}\cdot\mathbf{k}} \chi_{\frac{1}{2}\sigma_1}^{\dagger} \right.$$
$$\left. \times \Psi_D^{M_D\dagger}(\mathbf{r}) \Psi_{{\rm He}(H)}^{M_3}(\boldsymbol{\rho},\mathbf{r}) d\boldsymbol{\rho} d\mathbf{r} \right|^2 . \qquad (13)$$

Here, $\Psi_{{\rm He}(H)}^{M_3}(\boldsymbol{\rho},\mathbf{r})$ is the ^{3}He(^{3}H) ground-state wave function, M_3 the projection of the spin of ^{3}He (^{3}H), $\mathbf{r}$ and $\mathbf{rho}$ the Jacobi coordinates describing, respectively, the relative motion of the spectator pair and the motion of its c.m. with respect to the active nucleon "1". The second, excited (*ex*) part $P_{ex}^{p(n)}$ of $P_3(|\mathbf{k}_1|, E)$ in Eq. (10) corresponds to the three-body break-up (3bbu) channel $^3{\rm He}(^3{\rm H}) \to npp(n)$ and can be written, e.g., for the neutron spectral function in ^{3}He to be considered in this paper, as follows:

$$P_{ex}^{n}(|\mathbf{k}|, E) = \frac{1}{(2\pi)^3} \frac{1}{2} \sum_{M_3, S_{23}, \sigma_1} \int \frac{d^3\mathbf{t}}{(2\pi)^3}$$
$$\times \left| \int e^{-i\boldsymbol{\rho}\cdot\mathbf{k}} \chi_{\frac{1}{2}\sigma_1}^{\dagger} \Psi_{pp}^{\mathbf{t}\dagger}(\mathbf{r}) \Psi_{He}^{M_3}(\boldsymbol{\rho},\mathbf{r}) d\boldsymbol{\rho} d\mathbf{r} \right|^2$$
$$\times \delta\left(E - E_3 - \frac{\mathbf{t}^2}{m_N}\right), \qquad (14)$$

where $\Psi_{pp}^{\mathbf{t}}(\mathbf{r})$ is the two-body spectator continuum wave functions characterized by spin projection S_{23} and by the

relative momentum $\mathbf{t} = \frac{\mathbf{k}_2 - \mathbf{k}_3}{2}$ of the pp pair in the continuum. This definition of the SF, used in this and in other papers on the subject, is referred to as the *plane wave impulse approximation (PWIA)*, in which the continuum wave function of the spectator pair in the final state has to be chosen as the exact solution of the same Hamiltonian used to obtain the ground-state wave functions, with the motion of the active nucleon in the final state described by a plane wave; if, moreover, the interaction in the spectator pair is disregarded, with the three nucleons in the final state described by plane waves, one is referring to the so-called *plane wave approximation (PWA)*, a case which is relevant for the coming discussion. As a matter of fact, we are interested in the problem as to whether and to which extent the PWIA can be approximated by the PWA, since the microscopic model of the SF we are going to present implies the validity of the latter. In Fig. 1 two theoretical neutron SFs of ^{3}He are shown, namely the one obtained with a $3N$ variational wave function [15] corresponding to the Reid soft core (RSC) interaction [16], and the one obtained [17] using *ab initio* $3N$ wave functions [18] corresponding to the AV18 [19] NN interaction. It can be seen that, at high values of k and E^*, both SFs exhibit two common features, namely: (i) a peak located at values of the removal energy equal to $E \simeq k^2/4m_N$, and, more importantly, (ii) almost identical values around the peak of the PWIA and the PWA predictions, which means that around the peak the two-nucleon final state can safely be approximated by plane waves. This similarity between the PWIA and the PWA, which is illustrated in more detail in Fig. 2 in correspondence of several values of the momentum, will be shown in what follows to represent a clear manifestation of SRC.
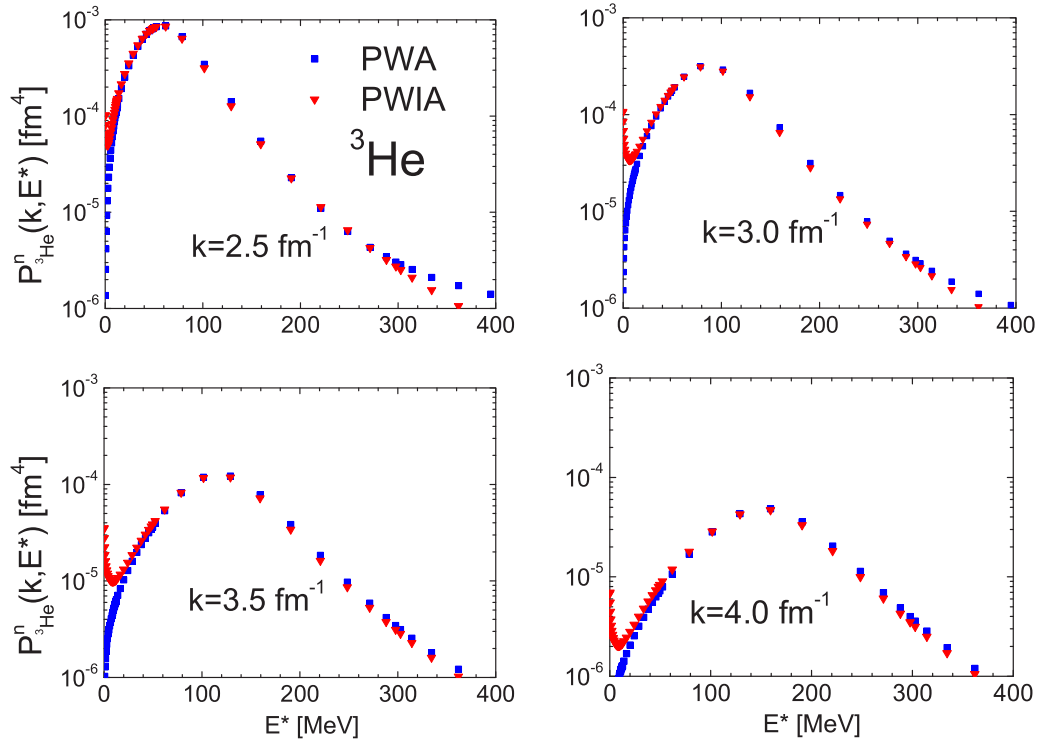
FIG. 2. The *ab initio* neutron spectral function of ^{3}He shown in Fig. 1(b) in correspondence of several values of the neutron momentum in PWA and PWIA, i.e., respectively, by disregarding (blue squares) and including (red triangles) the interaction in the *pp* final state. It can be seen that at high values of the neutron momentum ($k \gtrsim 2.5 \, \text{fm}^{-1}$) the final state interaction in the the *pp* essentially affects only the spectral function at small values of the excitation energy E^* (in this and the following figures $E^* = E_{\text{rel}}$).

III. THE KINEMATICS OF TWO- AND THREE- NUCLEON SRC

In this section it will be shown that different kinematical features of $2N$ and $3N$ SRC will differently affect the momentum and removal energy distributions of $P_{ex}^N(k, E)$.

A. 2N SRC

Momentum conservation in a system of A interacting nucleons implies that

$$\sum_{i=1}^{A} \mathbf{k}_i = 0 \qquad (15)$$

with the relative and c.m. momenta of a correlated nucleon-nucleon pair being

$$\mathbf{k}_{\text{rel}} = \frac{\mathbf{k}_1 - \mathbf{k}_2}{2} \quad \mathbf{K}_{\text{c.m.}} = \mathbf{k}_1 + \mathbf{k}_2 = -\sum_{i=3}^{A} \mathbf{k}_i \equiv -\mathbf{K}_{A-2}. \qquad (16)$$

It is a common practice to assume [20] that $2N$ SRC represent those configurations, depicted in Fig. 3(a), in which the active, high momentum nucleon "1" is correlated with the high momentum nucleon "2", with resulting "high" relative momentum $\mathbf{k}_{\text{rel}} = [\mathbf{k}_1 - \mathbf{k}_2]/2$, and "low" c.m. momentum $\mathbf{K}_{\text{c.m.}} = \mathbf{k}_1 + \mathbf{k}_2 = -\mathbf{K}_{A-2}$. Assuming that the $(A - 2)$

nucleus is left in its ground state, the intrinsic excitation energy of the $(A - 1)$-nucleon system E_{A-1}^* is given by the relative kinetic energy of the system composed by the second correlated nucleon N_2 (with momentum $\mathbf{k}_2$) and the $(A - 2)$-nucleon system (with momentum $\mathbf{K}_{A-2}$), namely,

$$E_{A-1}^* = \frac{1}{2 \, m_N} \frac{A-2}{A-1} \left[\mathbf{k}_2 - \frac{\mathbf{K}_{A-2}}{A-2} \right]^2 \xrightarrow{A=3} \frac{1}{m_N} \left(\frac{\mathbf{k}_2 - \mathbf{k}_3}{2} \right)^2. \qquad (17)$$

In the case of the so-called "naive 2NC model", which is the model based upon the assumption that $\mathbf{K}_{A-2} = 0$ ($\mathbf{k}_2 = -\mathbf{k}_1 \equiv -\mathbf{k}$) Eq. (17) trivially becomes

$$E_{A-1}^* = \frac{1}{2 \, m_N} \frac{A-2}{A-1} \mathbf{k}_2^2 \xrightarrow{A=3} \frac{\mathbf{k}^2}{4 m_N}. \qquad (18)$$

For the 3N systems, the main object of our investigations in the present paper, the residual nucleus is just the third *spectator* nucleon, so that the excitation energy of the $(A - 1)$-nucleon system is exactly the relative kinetic energy of particles "2" and "3", i.e., $k^2/(4 m_N)$, in agreement with the nonrelativistic *ab initio* calculation of the spectral function shown in Figs. 1 and 2.

B. 3N SRC

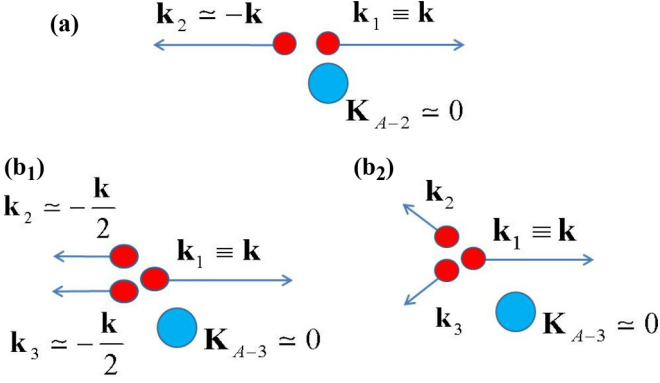When $3N$ SRC are at work, two limiting cases should be considered. In the first one [20], depicted in Fig. 3(b$_1$), the

FIG. 3. (a) Pictorial representation of the kinematics of $2N$ SRC in nucleus A: the high momentum $\mathbf{k}_1 \equiv \mathbf{k} \gtrsim 2.0\,\mathrm{fm}^{-1}$ of nucleon "1" is almost completely balanced by the momentum $\mathbf{k}_2 \simeq -\mathbf{k}$ of the correlated partner nucleon "2", with the residual system moving with low momentum $|\mathbf{K}_{A-2}| = |\mathbf{k}_1 + \mathbf{k}_2| \lesssim 1.0\,\mathrm{fm}^{-1}$. Momentum conservation reads as follows: $\sum_1^A \mathbf{k}_i = \mathbf{k}_1 + \mathbf{k}_2 + \mathbf{K}_{A-2} = 0$. In case of $A = 3$ the $(A - 2)$ nucleus is just a nucleon with momentum $\mathbf{K}_{A-2} = \mathbf{k}_3$. (b) Pictorial representation of the kinematics of $3N$ SRC in nucleus A. The three nucleons have high momenta and low c.m. momentum which is balanced by the momentum of the system $A - 3$. In the case of $A = 3$ the configuration in (b$_1$) can affect only the low removal energy part of the spectral function, whereas in the configuration (b$_2$) also the high removal energy part can be affected.

high momentum $\mathbf{k}$ of the active nucleon is balanced by two nucleons having almost equal momenta $\mathbf{k}/2$ antiparallel to $\mathbf{k}$; in such a configuration the excitation energy of $(A - 1)$ is trivially given by

$$E_{A-1}^* = \frac{A - 3}{A - 1} \frac{\mathbf{k}^2}{4\,m_N}, \tag{19}$$

which, obviously, vanishes for the three-nucleon system, being zero the relative momentum of particles "2" and "3". In the second, more general case depicted in Fig. 3(b$_2$), the excitation energy of $(A - 1)$ will be

$$E_{A-1}^* = \frac{1}{2\,m_N} \frac{A - 2}{A - 1} \left[\mathbf{k}_2 - \frac{\mathbf{K}_{A-2}}{A - 2}\right]^2$$
$$+ \frac{1}{2\,m_N} \frac{A - 3}{A - 2} \left[\mathbf{k}_3 - \frac{1}{A - 3}\mathbf{K}_{A-3}\right]^2$$
$$\xrightarrow{A=3} \frac{1}{m_N} \left[\frac{\mathbf{k}_2 - \mathbf{k}_3}{2}\right]^2. \tag{20}$$

Thus in the case of Fig. 3(b$_2$) the high momentum $\mathbf{k}$ of the active nucleon is balanced by two nucleons with high relative momentum $(\mathbf{k}_2 - \mathbf{k}_3)/2$, with resulting high excitation energy of $(A - 1)$ given by Eq. (20), and $3N$ SRC are expected to affect the high removal energy sector of the $3N$ spectral function in a way that will be illustrated in the next sections.

IV. FACTORIZATION OF THE MANY-BODY WAVE FUNCTION IN THE CORRELATIONS REGION AND THE CONVOLUTION STRUCTURE OF THE SPECTRAL FUNCTION AND MOMENTUM DISTRIBUTION

Factorization: The fundamental property of the nuclear wave function in the correlation region

As previously mentioned, several recent papers have argued [5–9] that at short internucleon relative distances the ground-state realistic many-body nuclear wave function Ψ_o exhibits the property of *factorization*, namely,

$$\lim_{r_{ij} \to 0} \Psi_0(\{r\}_A) \simeq \hat{A} \Bigg\{ \chi_o(\mathbf{R}_{ij}) \sum_{n, f_{A-2}} a_{o,n,f_{A-2}} [\Phi_n(x_{ij}, r_{ij})$$
$$\times \oplus \Psi_{f_{A-2}}(\{x\}_{A-2}, \{r\}_{A-2})] \Bigg\}, \tag{21}$$

which, in turns, is the origin of the presence of high momentum components [8,9].

In Eq. (21): (i) $\{r\}_A$ and $\{r\}_{A-2}$ denote the set of radial coordinates of nuclei A and $A - 2$, respectively; (ii) r_{ij} and $\mathbf{R}_{ij}$ are the relative and c.m. coordinate of the nucleon pair ij, described, respectively, by the relative wave function Φ_n and the c.m. wave function χ_o in $0s$ state; (iii) $\{x\}_{A-2}$ and x_{ij} denote the set of spin-isospin coordinates of the nucleus $(A - 2)$ and of the pair (ij). Factorized wave functions have been introduced in the past as physically sound approximations of the unknown nuclear wave function (see, e.g., [21]), without however providing any evidence of the validity of such an approximation due to the lack, at that time, of realistic solutions of the nuclear many-body problem which, however became recently available and the quantitative validity of the factorization approximation could be quantitatively checked. As a matter of fact the factorization property of realistic many-body wave functions has been proved to hold in the case of *ab initio* wave functions of few-nucleon systems [7] and in nuclear matter treated within the Brueckner-Bethe-Goldstone approach [6]. Moreover it has been shown [5] that the $2N$ momentum distribution in light nuclei in the region of *high* ($k_{\mathrm{rel}} \gtrsim 2\,\mathrm{fm}^{-1}$) relative momentum obeys indeed the property of factorization, i.e., it becomes independent upon the angle Θ between $\mathbf{k}_{\mathrm{rel}}$ and $\mathbf{K}_{\mathrm{c.m.}}$, namely,

$$n_A^{N_1 N_2}(\mathbf{k}_1, \mathbf{k}_2) = n_A^{N_1 N_2}(k_{\mathrm{rel}}, K_{\mathrm{c.m.}}, \Theta)$$
$$\simeq n_{\mathrm{rel}}^{N_1 N_2}(k_{\mathrm{rel}})\, n_{\mathrm{c.m.}}^{N_1 N_2}(K_{\mathrm{c.m.}}) \tag{22}$$

which, in the case of pn pairs, becomes

$$n_A^{pn}(k_{\mathrm{rel}}, K_{\mathrm{c.m.}}) \simeq C_A^{pn} n_D(k_{\mathrm{rel}})\, n_{\mathrm{c.m.}}^{pn}(K_{\mathrm{c.m.}}), \tag{23}$$

where n_D is the deuteron momentum distribution and C_A^{pn} is a constant depending upon the atomic weight and which, together with the integrals of $n_D(k_{\mathrm{rel}})$ and $n_{\mathrm{c.m.}}^{pn}(K_{\mathrm{c.m.}})$ in the proper SRC region, counts the number of SRC pn pairs in the given nucleus. It should be stressed that Eq. (23) is free from any adjustable parameters since all quantities appearing there result from many-body calculations [5]. It

should also be stressed that the results of Ref. [5] demonstrate that factorization is valid in the range of momenta including both low and high values of the c.m. momentum; in particular, as it will be quantified later on, the minimum value of the relative momentum at which factorization starts to occur is a function of the value of the c.m. momentum $K_{c.m.}$, namely factorization is valid when $k_{rel} \gtrsim k_{rel}^-(K_{c.m.})$, with [5]

$$k_{rel}^-(K_{c.m.}) \simeq a + b\,\phi(K_{c.m.}), \qquad (24)$$

where $a \simeq 2$ fm^{-1} and the function $\phi(K_{c.m.})$ is such that $\phi(0) \simeq 0$. The factorization of the momentum distributions leads to an interesting and physically sound interpretation, namely the region of *high* relative and *low* c.m. momenta is governed by $2N$ SRC, whereas the region in which also the c.m. momenta are *high* is governed by $3N$ SRC. Factorization leads to a peculiar relationship between the one- and two-nucleon momentum distributions in that the exact relation between the two quantities given by [8,9] ($N_1 \neq N_2$)

$$n_A^{N_1}(\mathbf{k}_1) = \frac{1}{A-1}\left[\int n_A^{N_1 N_2}(\mathbf{k}_1,\mathbf{k}_2)\,d\,\mathbf{k}_2 + 2\int n_A^{N_1 N_1}(\mathbf{k}_1,\mathbf{k}_2)\,d\,\mathbf{k}_2\right] \qquad (25)$$

can be expressed *in the factorization region* in terms of the following convolution integral $[\mathbf{k}_1 + \mathbf{k}_2 + \mathbf{k}_3 = 0,\ \mathbf{k}_3 = \mathbf{K}_{A-2} = -\mathbf{K}_{c.m.} = -(\mathbf{k}_1 + \mathbf{k}_2)]$ [5,8]:

$$n_A^{N_1}(\mathbf{k}_1) = \left[\int n_{rel}^{N_1 N_2}\left(\left|\mathbf{k}_1 - \frac{\mathbf{K}_{c.m.}}{2}\right|\right) n_{c.m.}^{N_1 N_2}(\mathbf{K}_{c.m.})\,d\,\mathbf{K}_{c.m.} + 2\int n_{rel}^{N_1 N_1}\left(\left|\mathbf{k}_1 - \frac{\mathbf{K}_{c.m.}}{2}\right|\right) n_{c.m.}^{N_1 N_1}(\mathbf{K}_{c.m.})\,d\,\mathbf{K}_{c.m.}\right]$$

$$\equiv n_{ex}^{N_1}(\mathbf{k}_1), \qquad (26)$$

so that the *correlation part* of the nucleon spectral function will be given by the following expression [5,8]:

$$P_1^{N_1}(\mathbf{k}_1, E) = \sum_{N_2 = p,n} C_{N_1 N_2} \int n_{rel}^{N_1 N_2}\left(\left|\mathbf{k}_1 - \frac{\mathbf{K}_{c.m.}}{2}\right|\right) n_{cm.}^{N_1 N_2}(\mathbf{K}_{c.m.})\,d\,\mathbf{K}_{c.m.}\,\delta\left(E - E_{thr} - \frac{A-2}{2m_N(A-1)}\left[\mathbf{k}_1 - \frac{(A-1)\mathbf{K}_{c.m.}}{A-2}\right]^2\right),$$

$$\qquad (27)$$

where $C_{N_1 = N_2} = 2$ and $C_{N_1 \neq N_2} = 1$. This is the *convolution model* of the spectral function which has been first obtained in Ref. [8] and applied there within the following approximations: (i) an effective two-nucleon momentum distribution for both pn and pp pairs has been used, and (ii) the constraint resulting from Eq. (31) has not been considered. The limits of validity of these approximations will be discussed in what follows and in a forthcoming paper devoted to complex nuclei. Moreover, up to now the convolution formula (27) has been applied assuming for the c.m. distribution a soft behavior in order to enhance the effects of $2N$ SRC involving low c.m. momentum components, which provides the largest contribution to the SRC peaks of the spectral function and to the high momentum part of the momentum distributions. In the present paper, following the finding of Ref. [5], demonstrating that factorization may also occurs at high values of the c.m. momentum (cf. Fig. 6 of Ref. [5]), we extend the factorization property to the treatment of $3N$ SRC and include in the convolution formula both the *soft* and the *hard* components of the c.m. momentum distributions, both resulting from *ab initio* many-body calculations, as illustrated in the next section in the case of the three-nucleon system.

V. $2N$ AND $3N$ SRC IN THE SPECTRAL FUNCTION OF ^{3}He

In this section the microscopic convolution model of the spectral function of the three-nucleon system embodying $2N$ and $3N$ SRC will be presented and compared with the *ab initio* spectral function. For ease of presentation we will discuss the neutron (proton) spectral function of ^{3}He (^{3}H), which requires

only the knowledge of the pn relative and c.m. momentum distributions.

A. The microscopic neutron spectral function of ^{3}He within the convolution model embodying $2N$ and $3N$ SRC

The basic ingredients to calculate the neutron spectral function in ^{3}He within the convolution model are the two-nucleon relative and c.m momentum distribution of the pn pair. Both quantities have been obtained in Refs. [19] and [22]; Fig. 4 shows the c.m. momentum distribution and it can be seen that the distribution can be split into a hard and a soft parts according to

$$n_{c.m.}^{pn}(K_{c.m.}) = n_{c.m.}^{pn,\text{soft}}(K_{c.m.}) + n_{c.m.}^{pn,\text{hard}}(K_{c.m.}). \qquad (28)$$

Thus, placing Eq. (28) in Eq. (27) the fully correlated neutron SF in ^{3}He (proton spectral function in ^{3}H) acquires the following form[1]:

$$P_{ex}^n(\mathbf{k}_1, E)$$

$$= \int n_{rel}^{np}\left(\left|\mathbf{k}_1 - \frac{\mathbf{K}_{c.m.}}{2}\right|\right)\left[n_{c.m.}^{np,\text{soft}}(K_{c.m.}) + n_{c.m.}^{np,\text{hard}}(K_{c.m.})\right]$$

$$\times d\,\mathbf{K}_{c.m.}\,\delta\left(E - E_{thr} - \frac{1}{4m_N}[\mathbf{k}_1 - 2\,\mathbf{K}_{c.m.}]^2\right). \qquad (29)$$

---

[1]Because of the lack of a bound nn state the sum in Eq. (27) extends only to free protons.
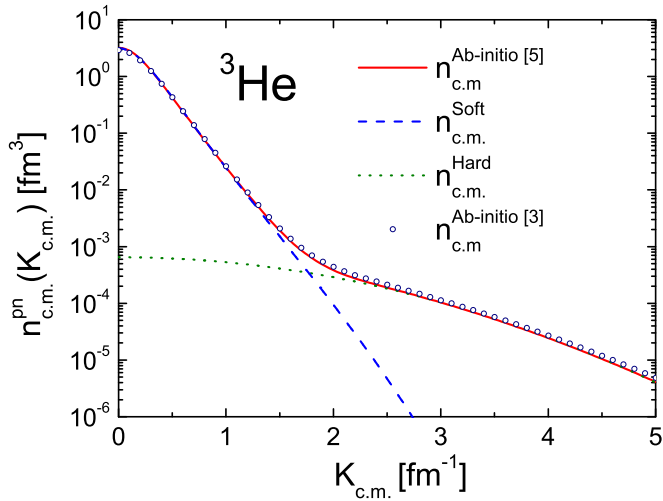
FIG. 4. The c.m. momentum distribution of the correlated proton-neutron pair in ^{3}He calculated in Ref. [5] (full line) and in Ref. [3] (open dots) with *ab initio* wave functions corresponding to the AV18 interaction. The figure shows the separation into the soft (dashed line) and hard (dotted line) components. (Adapted from Ref. [5].)

Here, we would like to reiterate that Eq. (29) represents a genuine parameter-free many-body quantity generated by *ab initio* relative and c.m. two-nucleon momentum distributions corresponding to a given local NN interaction. As a matter

of fact it should be remembered that the 2N relative and c.m. momentum distributions appearing there are nothing but the quantities obtained by using the one- and two-body many-body density matrices calculated with *ab initio* many-body wave functions. It is also worth stressing that Eqs. (27) and (29) are based upon the factorization property of the 3N wave function at short range, leading to the convolution model of the spectral function; for such a reason those equations are only valid in well defined ranges of the relative and c.m. momenta, which, in the present paper, are usually quantified as follows: the region in which $k_{rel}^- \geqslant 2 \, \text{fm}^{-1}$ and $K_{c.m.} \lesssim 1 \, \text{fm}^{-1}$ represents the 2N *SRC region*, whereas the region where $k_{rel}^- \geqslant 2 \, \text{fm}^{-1}$ and $K_{c.m.} > 1 \, \text{fm}^{-1}$ identifies the 3N SRC region. In Fig. 5 the k_{rel} dependence of the pn momentum distributions is shown in correspondence of several values of $K_{c.m.}$ and the region of factorization satisfying the relation

$$k_{rel} \geqslant k_{rel}^-(K_{c.m.}) \tag{30}$$

can be clearly identified as the region where the 2N momentum distributions corresponding to $\Theta = 0°$ and $\Theta = 90°$ overlap. Since the value of k_{rel}^- depends upon the value of $K_{c.m.}$, Eq. (30) generates a constraint on the region of integration over $\mathbf{K}_{c.m.}$ in Eq. (29), in that only those values of $\mathbf{K}_{c.m.}$ satisfying Eq. (30) have to be considered. Since for a fixed value of k_1 the relation between k_1 and $K_{c.m.}$ is given by

$$k_{rel} = \left| \mathbf{k}_1 - \frac{\mathbf{K}_{c.m.}}{2} \right| \geqslant k_{rel}^-(K_{c.m.}), \tag{31}$$
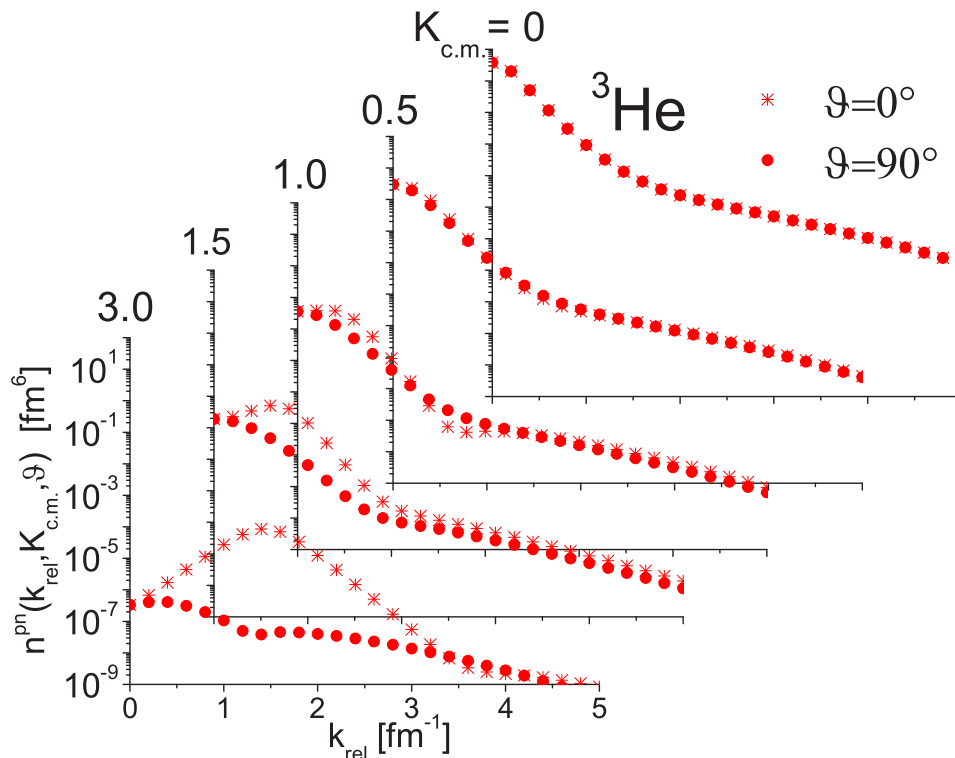

FIG. 5. The pn two-nucleon momentum distributions in ^{3}He, $n^{pn}(k_{rel}, K_{c.m.}, \theta)$, obtained *ab initio* in Ref. [5] in correspondence of several values of $K_{c.m.}$ and two values of the angle θ between $\mathbf{K}_{c.m.}$ and $\mathbf{k}_{rel}$. The region of k_{rel} where the value of $n^{pn}(k_{rel}, K_{c.m.}, \theta)$ is independent of the angle determines the region of factorization of the momentum distributions, i.e., $n^{pn}(k_{rel}, K_{c.m.}, \theta) \to n_{rel}^{pn}(k_{rel}) n_{c.m.}^{pn}(K_{c.m.})$. It can be seen that the region of factorization starts at values of $k_{rel} = k_{rel}^-$, which increase with increasing values of $K_{c.m.}$, i.e., $k_{rel}^- = k_{rel}^-(K_{c.m.})$; because of the dependence of k_{rel}^- upon $K_{c.m.}$, a constraint on the region of integration over $K_{c.m.}$ arises from Eq. (31). (Adapted from Ref. [5].)
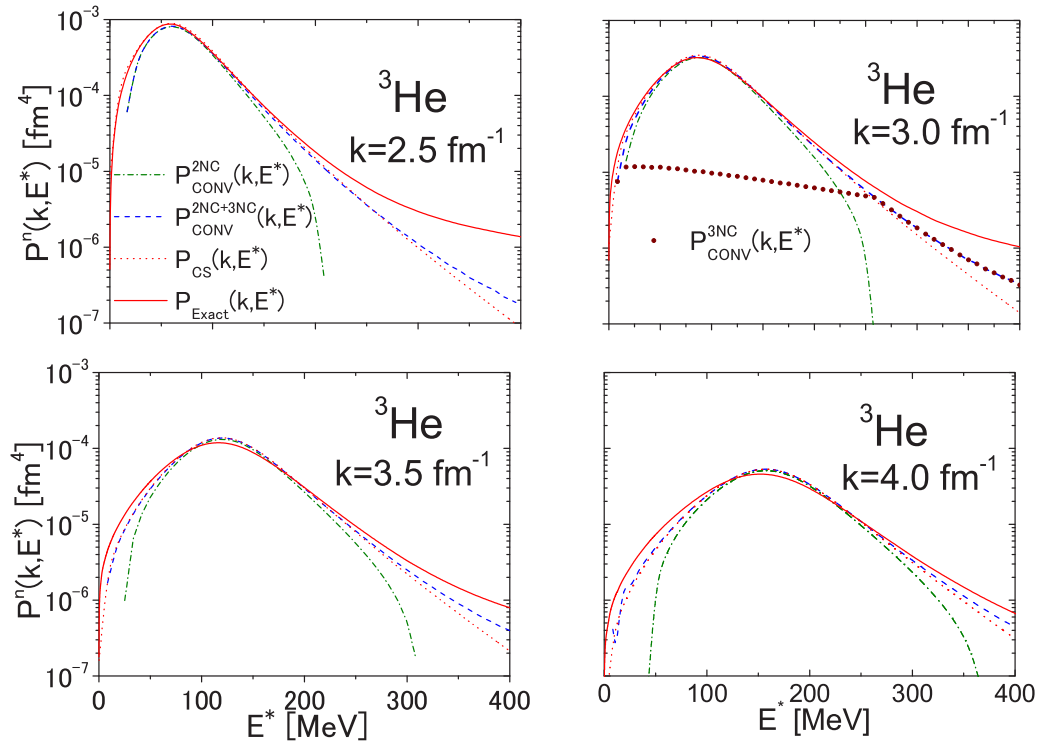
FIG. 6. Full line: the *ab initio* spectral function of the neutron in ^{3}He in PWA corresponding to the AV18 interaction, shown in Fig. 2 by the full squares. Dot-dashed line: convolution model which includes $2N$ SRC only ($k_{rel} > 2\,\text{fm}^{-1}$, $K_{c.m.} \leqslant 1.0\,\text{fm}^{-1}$); Dashed line: convolution model which includes both $2N$ ($k_{rel} > 2\,\text{fm}^{-1}$, $K_{c.m.} \leqslant 1.0\,\text{fm}^{-1}$) and $3N$ ($k_{rel} > 2\,\text{fm}^{-1}$, $K_{c.m.} > 1.0\,\text{fm}^{-1}$) SRC. Both dashed and dot-dashed lines include the constraint on the values of $K_{c.m.}$ imposed by the requirement of factorization [Eq. (31)]. Dotted line: convolution model of Ref. [8] which uses only the soft part of the c.m. momentum distribution without the constraint on the value of $K_{c.m.}$ [Eq. (31)]. The full dots in the case of $k = 3.0\,\text{fm}^{-1}$ denote the contribution from $3N$ SRC, i.e., the difference between the dashed and the dot-dashed curves.

this is the equation which establishes a constraint on the the region of integration over $\mathbf{K}_{c.m.}$; this region becomes narrower than the region which is obtained if the constraint given by Eq. (31) is disregarded. It is worth stressing that Eq. (31) and the resulting constraint were never been considered in the past.

B. The microscopic convolution model of the spectral function of ^{3}He embodying $2N$ and $3N$ SRC and its comparison with *ab initio* spectral functions

In this section the *ab initio* neutron spectral function of ^{3}He, [17], will be compared with the microscopic convolution model embodying $2N$ and $3N$ SRC calculated by Eq. (29) taking properly into account the constraint on the value of $K_{c.m.}$ imposed by Eq. (31), unlike what done in Ref. [8] where the constraint was not considered because the two-nucleon momentum distribution calculated at different angles was not known at that time. The result of these comparisons, in the region $2.5 < k < 4\,\text{fm}^{-1}$, $E \leqslant 400$ MeV, are shown in Fig. 6. A careful inspection at these results suggests the following comments:

(1) The prediction by the microscopic convolution model of the spectral function which correctly includes $2N$ SRC as previously defined ($k_{rel} \geqslant 2$ fm^{-1}, $K_{c.m.} \leqslant 1$ fm^{-1}), as well as the constraint resulting from Eq. (31) (dot-dashed line in Fig. 6), generally agrees with the

ab initio SF (full line), as far as the energy position of the peak, its amplitude and the energy region around it are concerned, but severely underestimates the high removal energy wings.

(2) The inclusion of $3N$ SRC, as previously defined ($k_{rel} \geqslant 2$ fm^{-1}, $K_{c.m.} > 1$ fm^{-1}), into the convolution model which satisfies Eq. (31) (dashed line) appreciably increases the amplitudes of the wings, leading to a satisfactory agreement with the *ab initio* spectral function, in a wide range of energy; the difference between the dashed and dot-dashed curves provides the effect of $3N$ SRC, whereas the difference between the full and the dashed curves identifies the region where the $3N$ configurations cannot be described by the factorized momentum distribution leading to the convolution model.

(3) The results within the model of Ref. [8] (dotted line), where only the soft part of the c.m. distribution is considered and the constraint on the values of $K_{c.m.}$ is disregarded, do not appreciably differ from the results obtained with the *ab initio* spectral function.

(4) The results shown in Fig. 6 can be explained as follows: (i) the hard part of the c.m. momentum distribution (dotted line in Fig. 4) produces a very high and unrealistic contribution to the spectral function (see Fig. 7) which is however cut down when the constraint [Eq. (31)] is taken into account; as a result, the amount
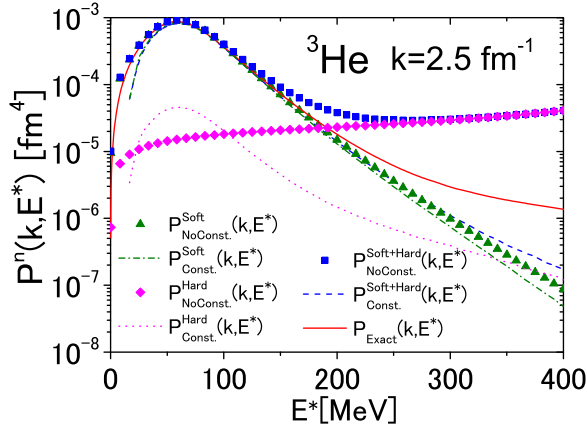
FIG. 7. The contributions to the neutron spectral function of the soft and hard parts of the c.m. momentum distributions shown in Fig. 4 in the case of $k = 2.5\,\mathrm{fm}^{-1}$ (cf. Fig. 6) considering (Const.) and disregarding (NoConst.) the constraint on the value of $K_{\mathrm{c.m.}}$ generated by Eq. (31).

of $3N$ SRC produced by the hard part of the c.m momentum distribution becomes comparable to the ones produced by the high momentum part of soft c.m momentum distribution; (ii) the sharp decrease of the $2N$ SRC contribution with increasing values of E^* is due to the fact that once the integration over the angle between $\mathbf{k}$ and $\mathbf{K}_{\mathrm{c.m.}}$ is carried out, the limits of integrations in $K_{\mathrm{c.m.}}$ in Eq. (29) are $K_{\mathrm{c.m.}}^- = |k - K_0|/2$ and $K_{\mathrm{c.m.}}^+ = (k + K_0)/2$, with $K_0 = (4 m_N E^*)^{1/2}$ and it can be trivially seen that beyond a certain value of E^*, which increases with increasing values of k, $2N$ SRC cannot occur, since they would fall outside the lower limits of integration.
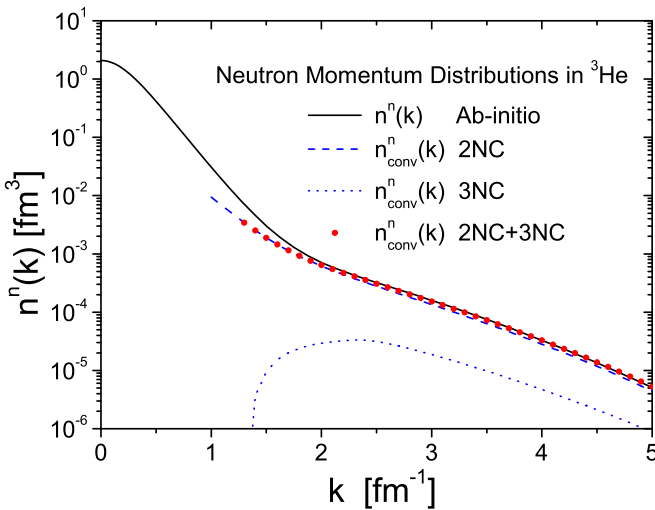

FIG. 8. The *ab initio* neutron momentum distribution in ^{3}He [22] (full line) compared in the high momentum region with the distribution obtained from the momentum sum rule [Eq. (6)], i.e., by integrating the convolution model spectral function [Eq. (27)]. Dotted line: contribution from $3N$ SRC; Dashed line: contribution from $2N$ SRC; Full dots: the sum of $2N$ and $3N$ SRC contributions.

(5) In the light of the previous remarks, it appears that in the case of ^{3}He the model of Ref. [8] effectively takes into account the factorization property of the two-body momentum distributions.

(6) In Fig. 8 the *ab initio* neutron momentum distribution $n_3^n(k)$ in ^{3}He (full line) is compared in the high momentum region with the distribution obtained from the momentum sum rule [Eq. (6)], i.e., by integrating the microscopic convolution model spectral function presented in Fig. 6; the dashed line includes only $2N$ SRC, whereas the full dots include both $2N$ and $3N$ SRC; it can be seen that although the contribution from $2N$ SRC is almost one order of magnitude higher than the one due to $3N$ SRC, the introduction of the latter brings the result of the microscopic convolution model in perfect agreement with the *ab initio* results.

VI. SUMMARY AND CONCLUSION

The main aspects and results of the present paper can be summarized as follows:

(1) We have reiterated that the basis of any treatment of SRC is the wave function factorization at short range leading in a natural way to the convolution model of the spectral function and, accordingly have developed an advanced microscopic many-body, parameter-free approach to the the nucleon spectral function expressed in terms of *ab initio* A-dependent two-nucleon relative and c.m. momentum distributions reflecting the underlying NN interaction; by this way we take into account the specific features of the given nucleus without recurring to approximations for finite nuclei relying on infinite nuclear matter.

(2) Unlike previous convolution models of the spectral functions, in our approach the region of factorization of the nuclear wave function in momentum space has been clearly identified and the resulting constraints on the values of the relative and c.m. momenta have been properly taken into account in the convolution integral.

(3) In the case of the three-nucleon system, we have found that when only $2N$ SRC are taken into account, the convolution model predictions agree within 80–90 % with the results of the *ab initio* spectral function as far as the peak position and the energy region around it are concerned, whereas far from the peak, particularly at high values of the removal energy, they disagree by orders of magnitude; this disagreement however is strongly reduced when one considers the effects of $3N$ SRC, which are implicitly generated by the high momentum part ($K_{\mathrm{c.m.}} > 1\ \mathrm{fm}^{-1}$) of the soft c.m. distribution used in the model of Ref. [8], or arise explicitly from the introduction of the hard components of the c.m. distribution as in Eq. (29) of the present paper; it turns out that the requirement of factorization lead to similar results in both cases; and whether such a result remains valid also in the case of complex nuclei is a current matter of investigations.

(4) We found that the high momentum part ($k \gtrsim 2\,\mathrm{fm}^{-1}$) of the neutron momentum distribution in ^{3}He is practically governed by the effects of $2N$ SRC, since the tails of the spectral function affected by $3N$ SRC have small effects on the energy removal integration; it should however be pointed out that the inclusion of $3N$ SRC brings the result of the microscopic convolution model in perfect agreement with the *ab initio* momentum distribution corresponding to the AV18 NN interaction.

To conclude, we would like to stress that by exploiting the universal factorization property exhibited by the short-range behavior of the nuclear wave function for finite nuclei, we have generated a microscopic and parameter-free spectral function based upon *ab initio* relative and center-of-mass two-nucleon momentum distributions for a given nucleus. The model rigorously satisfies the conditions for its validity, in that it takes into account only those two- and three-nucleon configurations

compatible with the requirement of wave function factorization. We have tested the convolution formula by a comparison with available *ab initio* spectral functions for the three-nucleon system resulting from the nonrelativistic Hamiltonian containing realistic local two-nucleon interactions (Argonne AV18), finding an excellent agreement in a wide range of removal energy and momentum, provided the effects of $3N$ SRC are also taken into account. It is highly satisfactory that such an agreement has been obtained without the use of any adjustable parameter. The generalization of our approach to complex nuclei, for which *ab initio* spectral functions cannot yet be obtained, is straightforward and will be presented elsewhere. We consider such a generalization particularly useful whenever precise calculations of nuclear effects in various processes, e.g., electron and neutrino scattering, is required. Needless to say that these type of processes require the inclusion of all types of final-state interaction which are at work when the active (struck) nucleon leaves the nucleus interacting with the spectator particles.

---

[1] L. Frankfurt, M. Sargsian, and M. Strikman, Int. J. Mod. Phys. A **23**, 2991 (2008); J. Arrington, D. W. Higinbotham, G. Rosner, and M. Sargsian, Prog. Part. Nucl. Phys. **67**, 898 (2012); O. Hen, D. W. Higinbotham, G. E. Miller, E. Piasetzky, and L. B. Weinstein, Int. J. Mod. Phys. E **22**, 1330017 (2013); M. Alvioli, C. Ciofi degli Atti, L. P. Kaptari, C. B. Mezzetti, and H. Morita, *ibid.* **22**, 1330021 (2013); C. Ciofi degli Atti, Phys. Rep. **590**, 1 (2015); O. Hen, G. A. Miller, E. Piasetzky, and L. B. Weinstein, arXiv:1611.09748v3 [nucl-ex] [Rev. Mod. Phys. (to be published)].

[2] E. Piasetzky, M. Sargsian, L. Frankfurt, M. Strikman, and J. W. Watson, Phys. Rev. Lett. **97**, 162504 (2006); R. Shneor *et al.* (Jefferson Lab Hall A Collaboration), *ibid.* **99**, 072501 (2007); R. Subedi *et al.*, Science **320**, 1476 (2008); O. Hen *et al.*, *ibid.* **346**, 614, (2014); Korover *et al.* (Lab Hall A Collaboration), Phys. Rev. Lett. **113**, 022501 (2014); O. Hen, E. Piasetzky, and L. B. Weinstein, Phys. Rev. C **85**, 047301 (2012).

[3] R. Schiavilla, R. B. Wiringa, S. C. Pieper, and J. Carlson, Phys. Rev. Lett. **98**, 132501 (2007); R. B. Wiringa, R. Schiavilla, S. C. Pieper, and J. Carlson, Phys. Rev. C **89**, 024305 (2014).

[4] D. Ding, A. Rios, H. Dussan, W. H. Dickoff, S. J. Witte, A. Carbone, and A. Polls, Phys. Rev. C **94**, 025802 (2016); J.-W. Chen, W. Dertmond, J. E. Lynn, and A. Schwenk, arXiv:1607.03065v1; J. Ryckebusch, M. Vanhalst, and W. Cosyn, J. Phys. G **42**, 055104 (2015); M. M. Sargsian, Phys. Rev. C **89**, 034305 (2014); O. Artiles, and M. M. Sargsian, *ibid.* **94**, 064318 (2016); A. Rios, A. Polls, and W. H. Dickhoff, *ibid.* **89**, 044303 (2014); H. Feldmeier, W. Horiuchi, T. Neff, and Y. Suzuki, *ibid.* **84**, 054003 (2011); L. B. Weinstein, E. Piasetzky, D. W. Higinbotham, J. Gomez, O. Hen, and R. Shneor, Phys. Rev. Lett. **106**, 052301 (2011); R. Roth, T. Neff, and H. Feldmeier, Prog. Part. Nucl. Phys. **65**, 50 (2010); Y. Suzuki and W. Horiuchi, Nucl. Phys. A **818**, 188 (2009).

[5] M. Alvioli, C. Ciofi degli Atti, and H. Morita, Phys. Rev. C **94**, 044309 (2016).

[6] M. Baldo, M. Borromeo, and C. Ciofi degli Atti, Nucl. Phys. A **604**, 429 (1996).

[7] C. Ciofi degli Atti, L. P. Kaptari, S. Scopetta, and H. Morita, Few-Body Syst. **50**, 243 (2011).

[8] C. Ciofi degli Atti and S. Simula, Phys. Rev. C **53**, 1689 (1996).

[9] R. Weiss, B. Bazak, and N. Barnea, Phys. Rev. C **92**, 054311 (2015); R. Weiss, R. Cruz-Torres, N. Barnea, E. Piasetzky, and O. Hen, arXiv:1612.00923v1[nucl-th] (2016).

[10] L. L. Frankfurt, M. I. Strikman, D. B. Day, and M. Sargsyan, Phys. Rev. C **48**, 2451 (1993).

[11] K. S. Egyian *et al.*, Phys. Rev. Lett. **96**, 082501 (2006).

[12] N. Fomin *et al.*, Phys. Rev. Lett. **108**, 092502 (2012).

[13] C. B. Mezzetti and C. Ciofi degli Atti, arXiv:0906.5564v1[nucl-th].

[14] W. H. Dickoff and D. V. van Neck, *Many-Body Theory Exposed* (World Scientific, Singapore, 2010).

[15] C. Ciofi degli Atti, E. Pace, and G. Salmè, Lect. Notes Phys. **86**, 316 (1978); Phys. Rev. C **21**, 805 (1980).

[16] R. V. Reid, Ann. Phys. (NY) **50**, 411 (1968).

[17] C. Ciofi degli Atti and L. P. Kaptari, Phys. Rev. C **71**, 024005 (2005).

[18] A. Kievsky, S. Rosati, and M. Viviani, Nucl. Phys. A **551**, 241 (1993).

[19] R. B. Wiringa, V. G. J. Stoks, and R. Schiavilla, Phys. Rev. C **51**, 38 (1995).

[20] L. L. Frankfurt and M. I. Strikman, Phys. Rep. **160**, 235 (1988).

[21] J. S. Levinger, Phys. Rev. **84**, 43 (1951).

[22] M. Alvioli, C. Ciofi degli Atti, L. P. Kaptari, C. B. Mezzetti, H. Morita, and S. Scopetta, Phys. Rev. C **85**, 021001(R) (2012).